Vietnam Journal of Biotechnology **22**(3): 507-522, 2024. DOI: 10.15625/vjbt-21211

REGULATION OF YEAST *RAD9* GENE IN ENERGY CHARGE, INTRACELLULAR ROS, AND CELL CYCLE ARREST IN RESPONSE TO DNA DAMAGE

Bui Van Ngoc[1,2]✉, Le Thanh Hoa[1,2]

[1]*Institute of Biotechnology (IBT), Vietnam Academy of Science and Technology (VAST), Hanoi, Vietnam.*

[2]*Graduate University of Science and Technology (GUST), VAST, Hanoi, Vietnam.*

✉To whom correspondence should be addressed. E-mail: bui@ibt.ac.vn

Received: 25.07.2024
Accepted: 24.09.2024

ABSTRACT

In various environmental conditions, eukaryotic cells are exposed to many kinds of exogenous toxic agents as well as to endogenous agents like reactive oxygen species (ROS) generated from oxidative metabolism that can all result in damage to DNA. To cope with these types of damage, yeast cells have evolved a number of mechanisms and specific response systems regulated by key control genes. One of which is *RAD9* gene that regulates DNA damage and repair checkpoints, and cell cycle arrest. Thus, a series of methods, e.g. oxygen consumption monitoring, physicochemical analysis, and flow cytometry, were used in the present study to investigate the role of the *RAD9* gene by using the BY4742 (wild type) and specific knock-out yeast strains (Δ*rad9*) and elucidate the function of this gene in cellular defense mechanism and metabolic response to DNA damage triggered by methyl methanesulfonate (MMS) treatment. The results indicated that fully functional DNA damage repair and cell cycle checkpoint (*RAD9*, wild type) significantly enhanced mitochondrial activity and oxygen consumption, reduced intracellular ROS accumulation. Fully functional mitochondria attenuated ROS accumulation, enabled efficient mitochondrial electron transport chain (mtETC) and ATP synthesis, and stabilized cellular energy status. Also, high mitochondrial activity acted as a protective mechanism against oxidative stress. In contrast, deletion of the *RAD9* (Δ*rad9*) resulted in high ROS accumulation and damaged to mitochondrial DNA, leading to strong inhibition of mitochondrial activity and oxygen consumption. Furthermore, low mitochondrial activity in cells lacking *RAD9* (Δ*rad9*) led to the development of oxidative stress. Subsequently, high ROS accumulation in Δ*rad9* cells caused a block of the mtETC, repression of ATP synthesis, fluctuation of cellular energy status, and induction of cell cycle arrest at S and G2/M phases.

Keywords: cell cycle arrest, DNA damage, MMS, ROS, RAD9, yeast

INTRODUCTION

During cell growth and proliferation, eukaryotic cells are exposed to many kinds of exogenous agents, including environmental mutagens and endogenous agents like reactive oxygen species (ROS)

from oxidative metabolism that can all result in damage to DNA. The ROS, such as superoxide anion radicals ($^{*}O_2^{-}$), hydroxyl free radicals ($^{*}OH$), and hydrogen peroxide (H_2O_2) are generated through both exogenous and endogenous routes and pose a significant threat to cellular integrity from damage to DNA, lipids, proteins, and other macromolecules (Salmon et al., 2004). Oxidative damage generated by intracellular ROS can lead to DNA base modification, single- and double-strand breaks (Canete et al., 2023; Waterman et al., 2020).

To cope with these kinds of DNA damage, yeast cells have evolved a number of defective cellular mechanisms, including DNA damage checkpoints, cell cycle arrest, stimulation of DNA repair (Yao et al., 2021), tolerance of DNA damage (Bellí et al., 2022), and initiation of apoptosis (Mihoubi et al., 2017; Ribeiro et al., 2006). DNA damage checkpoints are the signal transduction pathways that sense the presence of DNA damage and transmit a signal to downstream effectors to execute the various cellular responses to DNA damage. Cell cycle checkpoints recognize damage and arrest the cell cycle, or regulate transcriptional induction and progression of DNA replication (Dhingra et al., 2019; Pizzul et al., 2022).

Genes required for cell cycle arrest have been identified and reported in budding fission yeasts, and exert at least two functions: as sensors that associate with DNA and as signal transducers that mediate downstream events by phosphorylation (Canete et al., 2023; Dhingra et al., 2019). Of which the *RAD9* gene encodes Rad9, a DNA damage-dependent checkpoint protein. Rad9 is an adaptor protein required for cell cycle checkpoint function in *S. cerevisiae* and is a mediator of cell cycle arrest at the G_2/M cell cycle checkpoint induced by double-strand breaks (Schwarz et al., 2023). It is required throughout the cell cycle and has been shown to function at the G_1/S, intra-S, and G_2/M phases (Katheeja et al., 2021; Schwarz et al., 2023). Furthermore, Rad9 is required for activation of both Rad53 and Chk1 by the DNA damage checkpoint pathway. Additionally, Rad9 is a component of the Mec1/Rad9/Rad53 DNA damage repair pathway that controls mtDNA copying and mitochondrial stability (Katheeja et al., 2021; Navadgi-Patil & Burgers, 2008). Thus, Rad9 plays a role in controlling intracellular ROS levels and cell cycle arrest.

In mammalian cells, several proteins of damage checkpoint pathways also function as tumor suppressors, e.g. p53. Defects in checkpoint signaling pathways are frequently associated with cancer (Mello et al., 2017). Cellular responses to DNA damage, including cell cycle arrest, are a common feature of all eukaryotic cells and genes that mediate these responses are highly conserved. Many of the genes that regulate cell division in yeast were also shown to work similarly in humans (Guaragnella et al., 2014). The budding yeast *Saccharomyces cerevisiae* has long been recognized as a versatile model system for drug discovery and studying cellular defense in eukaryotic cells, since many of the basic cellular processes of both yeast and humans are also highly conserved. However, to date, no detailed analysis has been made to investigate the key gene that is crucial in DNA damage repair, cell cycle arrest and respiration in cellular response to DNA damage.

Thus, the aim of this study is to investigate the role of the *RAD9* gene that regulates DNA damage repair, intracellular ROS, and cell cycle arrest in *S. cerevisiae* in response

to DNA damage induced by DNA damaging agents. It is assumed that the intracellular ROS level probably depends on activation of the DNA damage repair pathway, namely the Mec1/Rad9/Rad53 DNA damage repair pathway that controls mtDNA copying and mitochondrial stability. The present study, therefore, uses the model yeast strain BY4742 (wild type) and the mutant Δ*rad9* that is defective in the *RAD9* gene deleted by the disruption of the respective gene to test these assumptions.

MATERIALS AND METHODS

Strains, media and growth conditions

Two yeast strains of *Saccharomyces cerevisiae* used in this study are BY4742 wild type (Accession number: Y10000; Genotype: *MATα; his3Δ1; leu2Δ0; lys2Δ0; ura3Δ0*; Source: EUROSCARF) and the mutant Δ*rad9* (Accession number: Y13576; Genotype: *MATα; his3Δ1; leu2Δ0; lys2Δ0; ura3Δ0; YDR217c::kanMX4*; Source: EUROSCARF). Yeast cells were grown in rich medium (YPD, Yeast Peptone Dextrose) containing 10 g/L yeast extract, 20 g/L bacto peptone, and 20 g/L glucose. Cell growth was followed by optical absorbance measurement at 600 nm (OD_{600}). For treatment with DNA-damaging agents, e.g. methyl methanesulfonate (MMS), medium was inoculated with overnight preculture and grown at 30˚C to the mid-log phase (OD_{600} values of 0.6–0.8). Then, cultures were either nontreated (control) or treated with MMS (Sigma-Aldrich) with different concentrations of 0.01%, 0.02%, and 0.04%.

OxoPlate® Assay

OxoPlate® (PreSens, Germany) was used to monitor oxygen consumption of cell growth in medium. Yeast cells were first inoculated in YPD medium, incubated at 30ºC/250 rpm/overnight (pre-culture), then pre-culture was transferred in fresh respective media YPD (main culture). Oxygen consumption (%) and cell growth ($OD6_{00}$) were monitored in 96-well OxoPlate® with round bottom integrated optical oxygen sensors, in which each well contained 75 µL of adjusted main culture (OD_{600} of 0.1) and 75 µL of MMS with investigated concentrations, 0.01%, 0.02%, and 0.04%, i.e. 150 µL in total.

The OxoPlate® was sealed with a breathable membrane (Diversified Biotech, USA), then introduced to the Tecan Safire^2 Reader (Tecan, Switzerland) to measure fluorescence intensity at 540/650 nm (for indicator dye, $I_{indicator}$) and 540/590 nm (for reference dye, $I_{reference}$), and at 600 nm (for optical density of culture, OD_{600}). The measurement was carried out continuously over 18 h with kinetic interval of 30 min at 30ºC. The calibration of the fluorescence reader was performed using a two-point calibration curve with oxygen free water (80 mM Na_2SO_3, *Cal 0*) and air-saturated water (*Cal 100*). Partial pressure of oxygen was calculated from the calibration curve.

Analysis of nucleotide content by HPIC

Metabolite extraction and sample preparation: The sampling preparation was described previously (Loret et al., 2007). Briefly, 20 units OD_{600} of cell culture were withdrawn at the indicated time point, rapidly collected by vacuum filtration (Glass Filter, Millipore™) through a Sartolon polyamide membrane (Sartorius, Germany). Cell-adherent membrane was quenched in 5 mL buffered ethanol (75% ethanol, 10 mM Hepes, pH 7.1) in 50 mL-glass tube (Lenz, Laborglas- instruments, Germany), shortly

vortexed, incubated at 85ºC/4 min in a water bath, and immediately put on ice. The membrane was then washed 2x0.5 mL with absolute ethanol to rinse the rest on the membrane in the solvent. The solvent containing cell extract suspension was evaporated to dryness at 35–40ºC under vacuum rotary around 35–50 mbar (Büchi, Rotavapor R, Switzerland). Cell extract was resuspended in 0.5 mL deionized water, centrifuged at 13000 rpm/4ºC/5 min. Supernatant was introduced to HPIC for analysis.

Analysis of nucleotide content: Supernatants (ca. 200 µL) were transferred into 1.5 mL-screw thread vials with glass inserts (VWR-™) and analyzed by High Performance Ion Exchange Chromatography (HPIC, Dionex – ICS – 3000, USA) equipped with a gradient pump and conductivity detector along with a UV detector (wavelength was set either to 220 or 260 nm). For the chromatographic separation, an AG11 guard column (50 mm × 2 mm i.d.) and 2 AS11 analytical columns (250 mm × 2 mm i.d.) (Dionex) in series were used. A flow of 0.35 ml/min was maintained throughout all runs. Suppressor current was set to 70 mA. The sample injection volume was 5 µL. The data was analyzed by Chromeleon software (Dionex, ICS – U3000). The content of metabolites and nucleotides was then quantified by Chromeleon software based on the calibration curve and calculated in µmol/g DW (dry weight). The analytical protocol follows the method described in Ritter (2006) (Ritter et al., 2006).

Calculation of energy charge: Energy charge, also called adenylate energy charge (AEC), is defined as the sum of hydrolysable phosphate bonds in adenine nucleotides over the total concentration of these nucleotides. Adenylate energy charge (AEC) is an index to estimate the cell energy status and calculated as proportional to the mole fraction of ATP plus half the mole fraction of ADP (Atkinson, 1968). The value of nucleotide levels was calculated in µmol/g DW and total intracellular adenine nucleotides AXP = (ATP + ADP + AMP). AEC was calculated as equal (ATP +1/2ADP)/(ATP + ADP + AMP).

Detection of ROS level, mitochondrial activity, and cell cycle arrest by flow cytometry

Preparation: Yeast cells were inoculated in YPD medium, incubated at 30ºC/250 rpm/overnight (pre-culture), then pre-culture was transferred in fresh YPD, incubated at 30ºC/250 rpm until mid-log phase (main culture). Main culture was split in two, one half culture as control (non-treated) and another one was treated with 0.03% MMS. Aliquots (ca. 50 – 100 µL) were taken at 3h, 6h, 8h and 24h after MMS treatment and mixed with ca 900 µL PBS (ca. 1 mL total). Aliquots were either stained with 50µM dihydroethidium (DHE, Molecular Probes, in final concentration – in f.c) for ROS detection or stained with 1 µM MitoTracker® Green FM (Molecular Probes – in f.c) plus 5 µg/mL of propidium iodide (PI, Sigma-Aldrich, in f.c) for mitochondrial activity detection. For cell cycle analysis, after centrifugation, the pellets were fixed in 70% ethanol at 4ºC for 24h, washed twice with ice-cold PBS and resuspended in 500 µL PBS. Cell suspensions were incubated with RNase A (50 µg/mL) for 30 min at 37ºC and sequentially stained with cold PI solution (50 µg/mL) in the dark for 1 h (Bui et al., 2024).

Flow cytometry analysis (fluorescence-activated cell sorting, FACS): FACS®

Calibur (Becton Dickinson) and CellQuest Pro analysis software were used to quantify and analyze fluorescence intensity of DHE, PI-DNA complex (excitation and emission settings were 488 and 564–606 nm, FL2 filter), and MitoTracker® (excitation and emission settings were 488 and 525–550 nm, FL1 filter). The analyzed fluorescence signal was given as the mean value of fluorescence intensity at the indicated time point (time course). One-Way ANOVA (analysis of variance) was used to determine the differences between the means by Excel and *p*–values < 0.05 were considered to be significantly different. The final graph performs overlapping histograms of fluorescence intensity against relative cell number according to time course. All assays and measurements were performed at least 3 times for reproducibility.

Modulation of oxygen consumption and cell growth in response to DNA damage

The ATP production and energy metabolism are directly dependent on oxygen consumption. Thus, the percentage of oxygen consumed in time (hours) together with cell growth expressed as OD_{600} were monitored and represented in Figure 1. The results indicate that DNA damage triggered by treatment with genotoxic chemical (MMS) caused adverse impairment of mitochondrial function of cells grown resulting in strong and rapid inhibition of oxygen consumption and cell growth at all investigated concentrations, especially mutant Δ*rad9* cells. MMS treatment significantly delayed oxygen consumption and cell proliferation in a dose-dependent manner (Figure 1).

RESULTS AND DISCUSSION

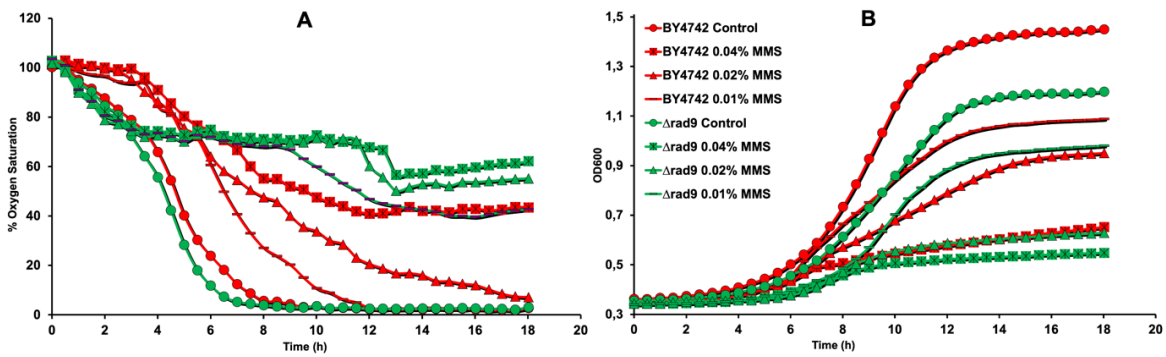

Figure 1. The kinetics of oxygen consumption (A) and cell growth (B) of the wild type BY4742 and the mutant Δ*rad9* upon treatment with MMS. The standard deviations of measurements were less than 5%, thus omitted. The legends in the growth curves (B) are also ones in the kinetics of oxygen consumption (A).

Afterward, mitochondrial function was either recovered until oxygen in the medium became exhausted or remained inhibited, i.e. no more oxygen was consumed. Indeed, cells lacking the *RAD9* gene consumed up to 50% of oxygen in the medium due to treatment with 0.01–0.04% MMS (green lines, Figure 1A), while the wild type consumed around 50% of oxygen even treated with the highest MMS concentration and was able to regain mitochondrial activity and continue oxygen consumption at lower

treated MMS concentrations until oxygen depleted (red lines, Figure 1A). Mutant Δ*rad9* cells were much more susceptible to MMS treatment and showed stronger enhancement of mitochondrial respiratory block, leading to a more rapid decrease in oxygen consumption and subsequent lower exponential growth rate compared with wild types (Figure 1, A). The mutant cells were not able to regain mitochondrial function, resume oxygen consumption, and continue cell proliferation when exposed to genotoxic chemical as the wild type could.

Thus, fully functional DNA damage checkpoint pathways play an important role in response to oxidative stress and DNA damage. The recovery of mitochondrial function and oxygen consumption as well as the increase of cell growth depend on the activity of some key genes which play an important role in DNA damage checkpoint pathway and cell cycle arrest, e.g *RAD9*. Indeed, disruption of the DNA damage checkpoint and cell cycle arrest at the G1/S, intra-S, and G2/M phases by deletion of *RAD9* gene (Δ*rad9*) strongly impaired mitochondrial function, mitochondrial electron transport chain (mtETC) or mitochondrial activity, and inhibited oxygen consumption (Katheeja et al., 2021; Schwarz et al., 2023; Sjölander & Sunnerhagen, 2020).

Changes in mitochondrial activity in response to DNA damage

Mitochondrial activity of controls of BY4742 and Δ*rad9* started to decrease at the beginning of cultivation and was slightly higher at around 8 h, then started to decrease again up to 24h. It could be explained that when glucose was available in full medium (YPD) within 3 h, fermentation rather than respiration was preferred, resulting in low mitochondrial activity. When glucose was completely exhausted at around 6–8 h of cultivation, respiration was preferred, and subsequently mitochondrial activity increased (Figure 2). Mitochondrial activity of the wild type cells is higher than that of the mutant cells from 6 h (at the time of glucose depletion) until 24h of cultivation. Due to the high mitochondrial activity of the wild type, this was able to recover mitochondrial functions and regain oxygen consumption faster and increase cell survival better than the mutant (Figure 2).

The observed effects on mitochondrial activity and consequent oxygen consumption probably result from mitochondrial DNA (mtDNA) damage triggered by genotoxic chemical treatment that induces high ROS accumulation and further impairs mtETC or mitochondrial activity. Since mtDNA might be more prone to oxidative damage and suffers 3–10 fold more damage than nuclear DNA (nDNA) in numerous cell types from yeast, mouse, rats, and humans (Chenna et al., 2022; Van Houten et al., 2006), it is also particularly susceptible to ROS generated by the mtECT (Shokolenko et al., 2009).

So, what caused inhibition of mitochondrial activity? As mentioned, mtDNA is the preferred target for MMS-mediated DNA damage (Kitanovic et al., 2009), i.e. MMS treatment causes mtDNA damage, inhibition of the mitochondrial electron transport chain, and subsequent increase of ROS accumulation. MtDNA seems to be a critical target for such oxidative damage and is particularly susceptible to ROS generated by the mitochondrial electron transport chain due to its close proximity (Senoo et al., 2016; Stenberg et al., 2022). Thus, the ROS

level resulting from MMS treatment was further investigated.

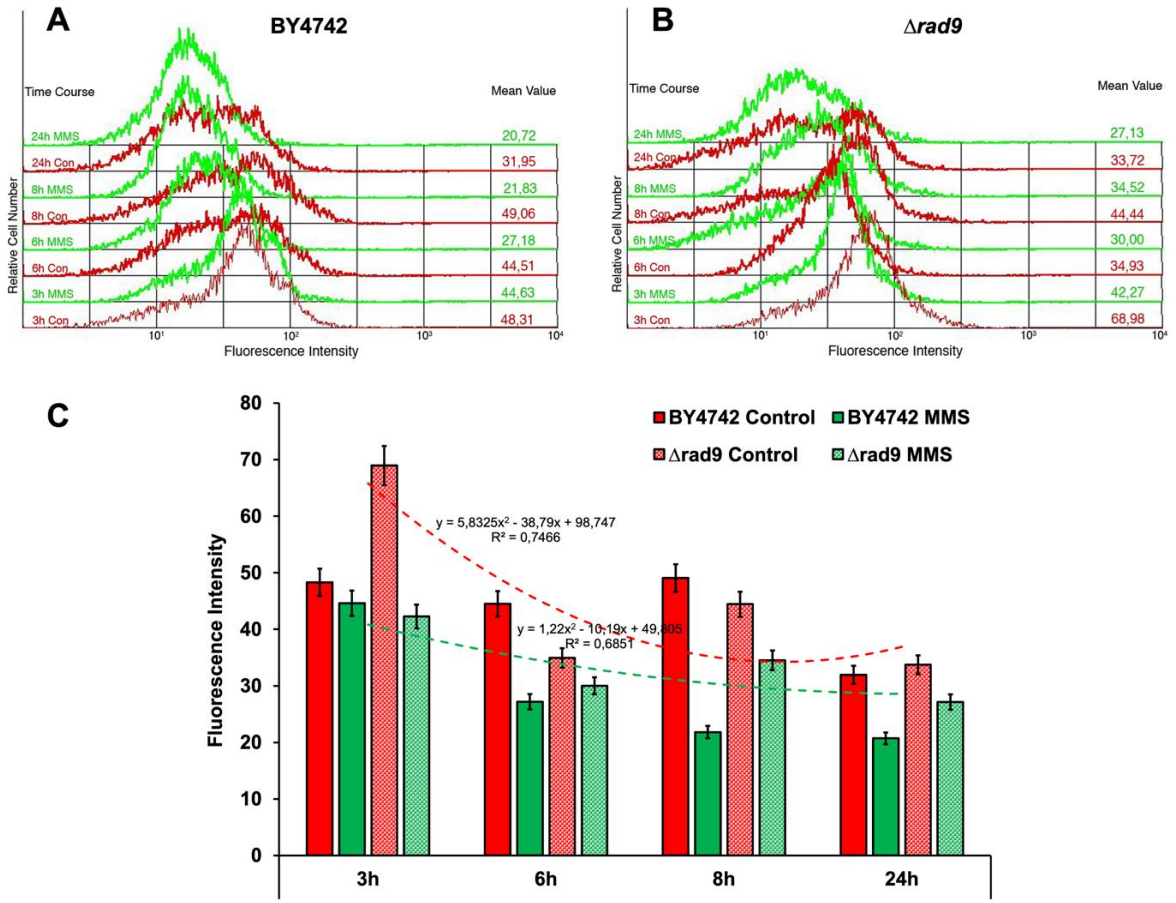

Figure 2. Modulation of mitochondrial activity of BY4742 (A) and Δ*rad9* (B) in response to DNA damage. Fluorescence intensity was quantified and analyzed by FACS for measuring mitochondrial activity; results are given as mean values. Graphs represent the mean value of fluorescence intensity measured at each time point when aliquots were taken at 3h, 6h, 8h, and 24h. The dashed lines with quadratic equations represent the trends of mitochondrial activity during 24h of cultivation (C).

Inhibition of mitochondrial activity leads to high ROS accumulation

Since ROS is generated by the mitochondrial electron transport chain (mtETC) even during normal metabolism (Whalley et al., 2018), ROS generation correlates with high oxygen consumption and exponential growth rate. High ROS levels could be produced in mutants that are defective in DNA damage repair and cell cycle arrest, such as Δ*rad9* or in cells exposed to DNA damaging agents like MMS.

As assumed, ROS levels of all MMS-treated cultures gradually increased throughout the cultivation period. However, ROS levels of control YPD cultures dramatically increased at around 6–8 h during log-phase, reaching a maximum at 8 h, then starting to decrease in the stationary phase as glucose in the medium is completely exhausted (Figure 3).

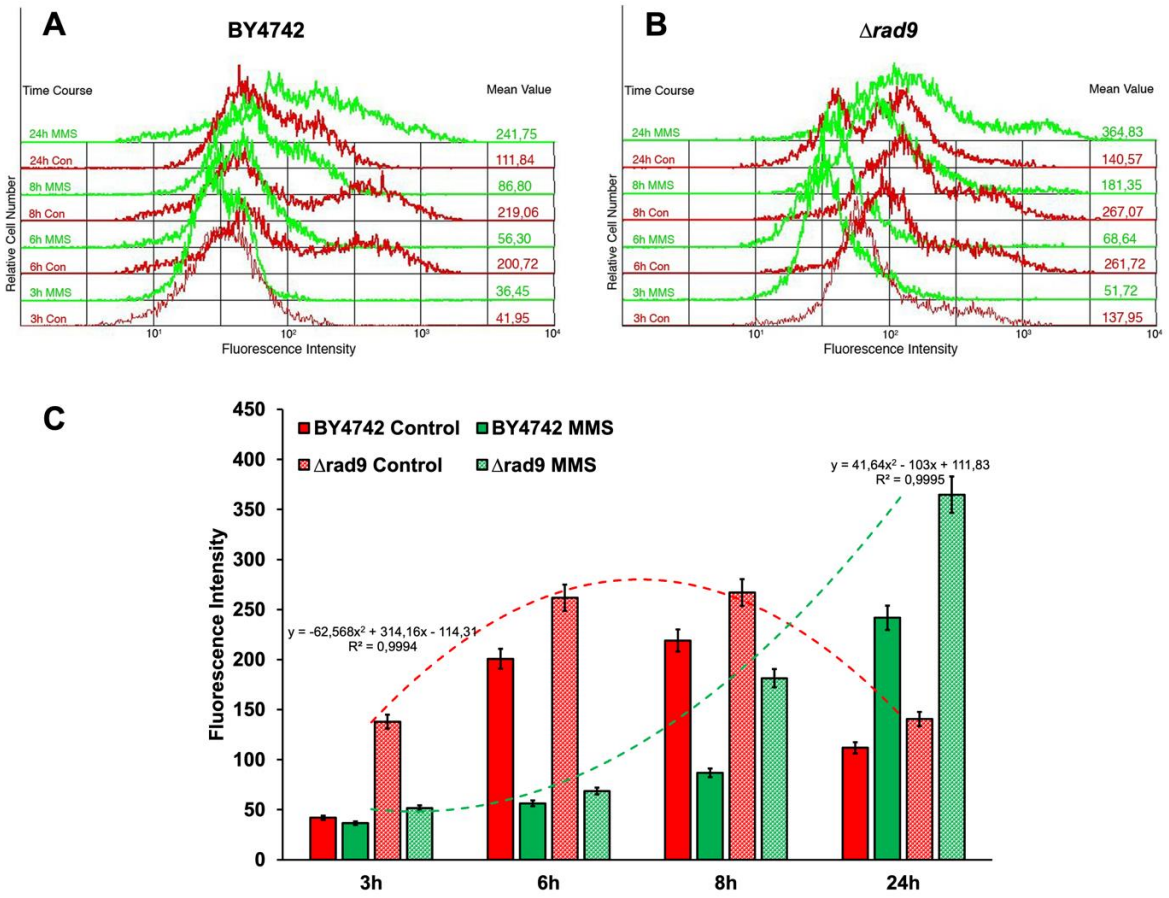

Figure 3. ROS accumulation of BY4742 (A) and Δ*rad9* (B) in response to DNA damage. Fluorescence intensity was quantified and analyzed by FACS for determining ROS level, results are given as mean values. Graphs represent the mean value of fluorescence intensity measured at each time point when aliquots were taken at 3h, 6h, 8h, and 24h. The dashed lines with quadratic equations represent the trends of ROS accumulation during 24h of cultivation (C).

Disruption of *RAD9* (Δ*rad9*) led to high ROS levels in untreated control cultures when compared to control cultures of the wild type. Δ*rad9* cells in particular generated high ROS levels in both MMS-treated cultures as compared with all wild-type (Figure 3). The results suggest that a lack of DNA damage repair pathways and cell cycle checkpoints causes high ROS accumulation even in normal metabolism or in exposure to DNA damaging agents.

Because oxidative stress from ROS (reactive oxygen species) affects replication and transcription of mtDNA (Cui et al., 2012) and causes damage to DNA by chemical modification (Kurita et al., 2020). DNA damage impairs genome stability, proper chromosomal segregation and cell viability, and H_2O_2 induces both single- and double-strand breaks (Ribeiro et al., 2006). MMS is an alkylating agent and carcinogen, it methylates N^7-deoxyguanine and N^3-deoxyadenine bases of DNA, directly causing double-strand breaks and stalling replication forks (Groth et al., 2010). Thus,

RAD9 plays a crucial role in controlling intracellular ROS levels.

In essence, MMS treatment could damage mtDNA resulting in inhibition of the mitochondrial electron transport chain with a subsequent increase of ROS level. So, how does ATP synthesis respond to DNA damage? Does the ATP production and energy status increase or decrease in response to DNA damage? Further investigations were continued to address these questions.

Inhibition of mitochondrial activity leads to reduced ATP synthesis and energy status

Earlier findings suggest that DNA damage induced by MMS impairs mitochondrial activity as a result of ROS accumulation (Figure 2–3). It is possible that this causes inhibition of ATP synthesis.

Furthermore, many reactions in metabolism are controlled by the energy status of the cell. One index of the energy status is the energy charge, also called adenylate energy charge (AEC), which is proportional to the mole fraction of ATP plus half the mole fraction of ADP defined as equal (ATP + 1/2ADP)/(ATP + ADP + AMP) (Atkinson, 1968). Thus, AEC depends on the relative amounts of ATP, ADP, and AMP and can have a value ranging from 0 (all AMP) to 1 (all ATP). A high energy charge inhibits ATP synthesis (catabolic pathways), but it stimulates ATP utilization (anabolic pathways) and vice versa (Berg et al., 2002a). The total adenine nucleotides (AXP) is defined as equal (ATP + ADP + AMP).

MMS treatment inhibits ATP synthesis of both the wild type and Δ*rad9* already after 3 h of treatment resulting in a reduction of ATP levels as compared to controls (Figure 4, panels A, B). This decrease of ATP levels in MMS-treated conditions also contributed to the decrease of total adenine nucleotides (AXP) and AEC over time compared to controls (Figure 4, panels C, D).

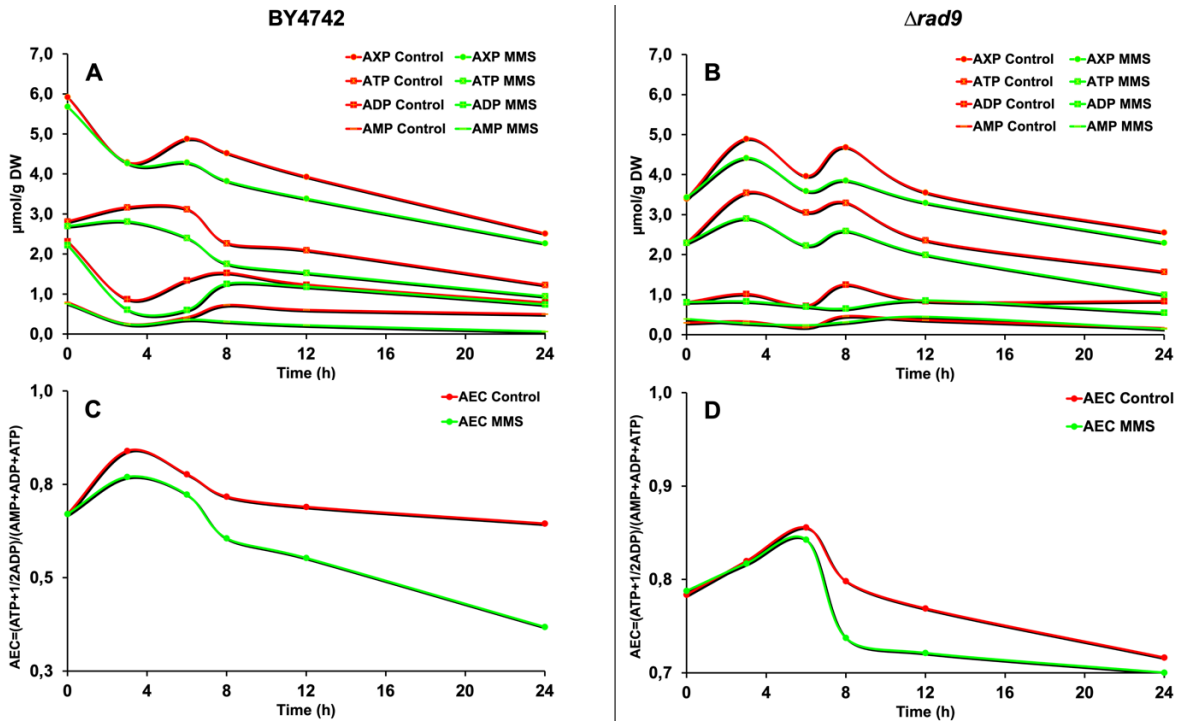

Figure 4. Changes in ATP, ADP, AMP levels and adenylate energy charge (AEC) in response to DNA damage. Intracellular metabolite extracts were analyzed by HPIC at each time point taking aliquots at 3h, 6h, 8h, and 24h. The value of nucleotide levels was calculated in µmol/g DW (dry weight) (panels A, B) and total intracellular adenine nucleotides AXP = (ATP + ADP + AMP). AEC was calculated as equal (ATP +1/2ADP)/(ATP + ADP + AMP) (panels C, D).

The increase of AEC during the first hours in the BY4742 control culture (0–3 h) resulted from the increase of cellular ATP levels which indicates that cells have not yet required a large number of building blocks such as amino acids and nucleotides nor a large amount of energy for cell proliferation. In this case, high AEC inhibits catabolism leading to a reduction of ADP and AMP levels, and a subsequent decrease in total intracellular adenine nucleotides (AXP) at this stage (Figure 4, panels A, C).

However, from 3–8 h (mid-log and log phases) AEC significantly decreased. In this case, low AEC stimulates ATP synthesis (catabolism), but simultaneously stimulates ATP consumption (anabolism) used for DNA/RNA synthesis leading to the generation of ADP and AMP in this stage (Figure 4, panels A, C). Thus, in this log-phase cells required a large amount of energy used for exponential growth leading to a decease of the cellular ATP pool. From 8 h AEC was nearly invariable, i.e. the energy status of cells was balanced (Figure 4, C). In this stationary phase, there is a balance between catabolism and anabolism, cells cease to divide in response to nutrient limitations, while in the control culture of Δ*rad9,* the AXP pool and AEC seem to depend on changes in ATP levels.

Nevertheless, in both the MMS-treated cultures of the wild type and Δ*rad9*, AEC was strongly reduced and significantly lower than that in controls (Figure 4, C, D). Since ATP synthesis was inhibited as a result of

impaired mitochondrial activity and metabolic flux was re-routed towards early stages of glycolysis, leading to lower ATP levels, the AECs decreased.

Thus, MMS-treated cells were not able to maintain their energy balance as compared to untreated cells (controls). The inhibition of ATP synthesis over time contributes to the decrease of total adenine nucleotides (AXP) and subsequent adenylate energy charge (AEC) of both MMS-treated BY4742 and Δ*rad9* cells. The reduced AEC over time will affect a balance between catabolism and anabolism of cells. Since the AEC value reflects balance between catabolic and anabolic pathways and depends on the relative amounts of ATP, ADP, and AMP. A high AEC value inhibits ATP synthesis (catabolic pathways), but stimulates ATP utilization (anabolic pathways) and vice versa (Berg et al., 2002b).

So, cells lacking the DNA damage checkpoint and cell cycle arrest by deletion of *RAD9* gene (Δ*rad9*) result in high ROS accumulation, thereby increasing damage to mtDNA and leading to inhibition of mitochondrial activity and oxygen consumption. Further experiment was proceeded to determine whether cell cycle arrest was induced by MMS treatment at the G1/S, intra-S, or G2/M phases.

Induction of cell cycle arrest in response to DNA damage

To further explore the MMS-induced distribution of cells in the cell cycle phases, the MMS-treated cells were incubated with RNase A and stained with PI to form PI–DNA complex. The relative DNA content (%) estimated as the emitted fluorescence of PI was then measured by FACS. The flow cytometric results indicated that accumulation of both cells, BY4742 and Δ*rad9*, was detected at S and G2/M phases (Figure 5), implying an accompanying cell cycle arrest and the existence of a block at these phases of the cell cycle. Furthermore, MMS treatment induced more cells to accumulate at S and G2/M phases of the cell cycle as compared with the control (non-treated), whereas it triggered fewer cells to accumulate at the G1 phase than the controls. Also, Δ*rad9* cells were accumulated at S and G2/M phases more than BY4742 ones (Figure 5).

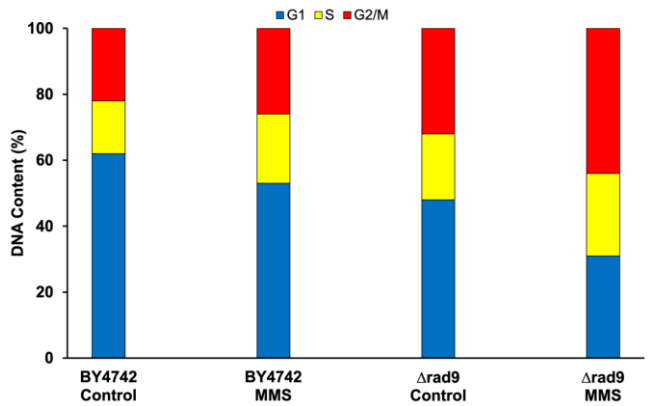

Figure 5. Induction of cell cycle arrest by MMS treatment. Phase cell arrest was determined by FACS using a PI staining of relative DNA content. All measurements were performed at least 3 times for reproducibility.

Thus, these results revealed that high ROS accumulation led to activation of cell cycle arrest at the S and G2/M phases that blocked the DNA synthesis and inhibited cell growth as the cellular defense mechanism. Indeed, the high ROS accumulation is linked to activation of DNA damage repair pathways, in particular the Mec1/Rad9/Rad53 DNA damage repair pathway that controls mtDNA copying and mitochondrial stability (Katheeja et al., 2021; Navadgi-Patil & Burgers, 2008). Moreover, these findings agree with previous reports said that MMS treatment induced cell cycle arrest at S and G2/M phases in yeast (Katheeja et al., 2021; Siler et al., 2017). Additionally, regulation of the cell cycle by Δ*rad9* was eliminated by radiation, and Δ*rad9* exhibited a 20-fold increase in the rate of chromosome loss in the absence of any extrinsic DNA damage (Bierle et al., 2015; Hartwell, 2002; Hu et al., 2008). This suggests that the checkpoint function is needed in those cells to assure correct repair of the damage and such defects may be manipulated in mammalian cells as well.

The relationship between checkpoints and cancer was established through studies of two human genes, *p53* and *ATM*. Both genes have additional roles in other cellular responses to DNA damage, such as apoptosis and transcriptional regulation. The *p53* gene is a tumor suppressor found to be mutated in half of all human cancers (Marei et al., 2021). The *ATM* mutation leads to complex phenotypes culminating in death in the second or third decade of life (van Os et al., 2020) . The checkpoint defects in cancer cells may be useful in designing new cancer therapy strategies. Indeed, the findings in this study show that checkpoint defects in yeast cells lead to increased sensitivity to DNA damaging agents. Defects in checkpoint signaling pathways, cell cycle arrest are frequently associated with cancer (Dixon & Norbury, 2002; Engeland, 2018) and are a common feature of all eukaryotic cells. Many of the genes that regulate cell division in yeast also act similarly in humans, e.g. cell division cycle (*CDC*), cyclin-dependent kinase 1 (*CDK1*), and DNA repair and checkpoint genes (*RAD9*) in *S. cerevisiae* (Ferrari et al., 2020). Thus, the role of other genes regulating DNA damage checkpoints and cell cycle arrest like *RAD53*, *CDK1* or *MEC1* should be examined in further works.

CONCLUSION

In summary, the above findings indicate that the specific response of the individual mutant strain Δ*rad9* elucidates the role of the corresponding gene depicted by the respective pathway in response to DNA damage (Figure 6). Indeed, fully functional DNA damage repair and cell cycle checkpoint (*RAD9*, wild type) significantly reduces intracellular ROS accumulation, defects of *RAD9* (Δ*rad9*, mutant) result in high ROS accumulation, thereby increasing damage to mtDNA and leading to reduced mitochondrial activity and oxygen consumption. Subsequently, lack of *RAD9* (Δ*rad9*) causes blockage of mtETC, repression of ATP synthesis, and fluctuation of cellular energy status (AEC). Taken together, high mitochondrial activity (wild type) reduces the development of oxidative stress and acts as a protective mechanism against oxidative stress, low mitochondrial activity (Δ*rad9*) can lead to enhanced ROS accumulation and induction of cell cycle arrest at S and G2/M phases (Figure 6).

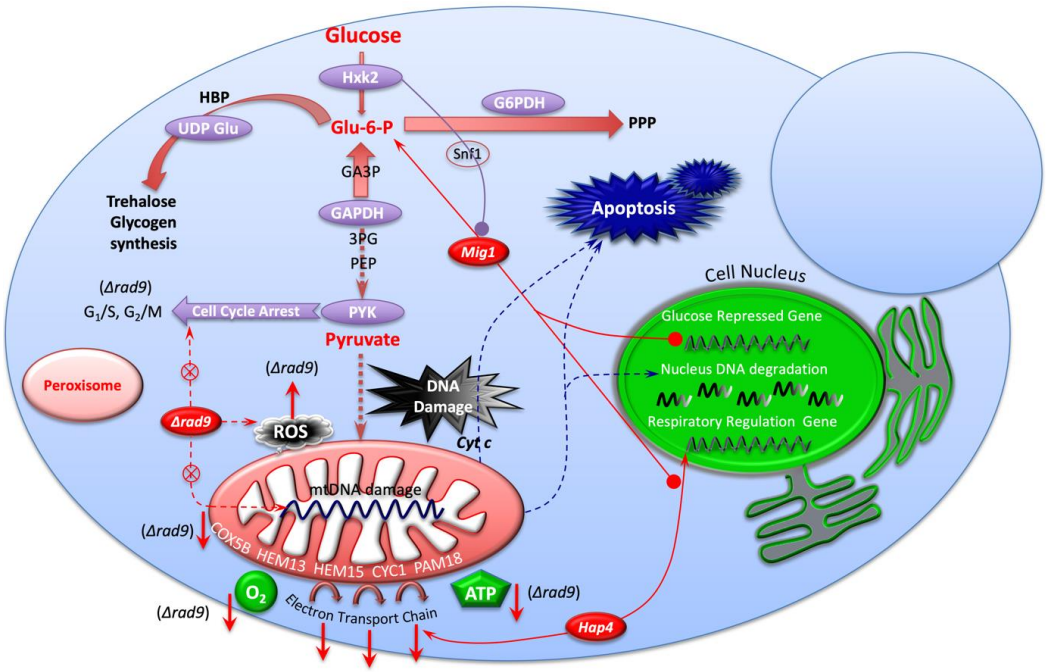

Figure 6. Schematic summary of the role of the yeast *RAD9* gene in energy charge, intracellular ROS, and cell cycle arrest in response to DNA damage. Treatment of DNA damage agents (MMS) strongly inhibit mitochondrial electron transport chain – mtETC (perhaps because of damaging mtDNA) and decreases oxygen consumption of Δ*rad9*. MMS treatment induced high ROS accumulation, especially in mutants defective in cell cycle arrest and control of mtDNA copying, Δ*rad9*. Further effect is the inhibition of ATP synthesis. Also, ROS directly inhibit mitochondrial activity leading to the initiation of cell cycle arrest at S and G2/M phases.

CONFLICT OF INTEREST

The authors declare that there is no conflict of interest.

ACKNOWLEDGMENT

We thank Stefan Wölfl, Ana Kitanovic for valuable comments regarding the experiments and sharing ideas regarding data analysis. This work was supported by the SysMO Project Network (EU-BMBF) on Systems Biology of Microorganisms (MOSES, WP 4.3, S.W. and A.K.).

REFERENCES

Atkinson, D. E. (1968). The Energy Charge of the Adenylate Pool as a Regulatory Parameter. Interaction with Feedback Modifiers. *Biochemistry*, *7*(11), 4030–4034. https://doi.org/10.1021/bi00851a033

Bellí, G., Colomina, N., Castells-Roca, L., & Lorite, N. P. (2022). Post-Translational Modifications of PCNA: Guiding for the Best DNA Damage Tolerance Choice. *J. Fungi*, *8*(6), 621. https://doi.org/10.3390/jof8060621

Berg, J., Tymoczko, J., & Stryer, L. (2002a). Biochemistry. 5th Edition, New York: W H Freeman. In *New York: W H Freeman*.

Berg, J., Tymoczko, J., & Stryer, L. (2002b). Biochemistry. 5th Edition, New York: W H Freeman. In *New York W H Free.*

Bierle, L. A., Reich, K. L., Taylor, B. E., Blatt, E. B., Middleton, S. M., Burke, S. D., Stultz, L. K., Hanson, P. K., Partridge, J. F., & Miller, M. E. (2015). DNA damage response checkpoint

activation drives KP1019 dependent pre-anaphase cell cycle delay in S. cerevisiae. *PLoS One*, *10*(9), e0138085. https://doi.org/10.1371/journal.pone.0138085

Bui, V. N., Nguyen, T. P. T., Nguyen, H. D., Phi, Q. T., Nguyen, T. N., & Chu, H. H. (2024). Bioactivity responses to changes in mucus-associated bacterial composition between healthy and bleached Porites lobata corals. *J. Invertebr. Pathol.*, *206*, 108164. https://doi.org/10.1016/j.jip.2024.108164

Canete, J. A., Andrés, S., Muñoz, S., Zamarreño, J., Rodríguez, S., Díaz-Cuervo, H., Bueno, A., & Sacristán, M. P. (2023). Fission yeast Cdc14-like phosphatase Flp1/Clp1 modulates the transcriptional response to oxidative stress. *Sci. Rep.*, *13*(1), 14677. https://doi.org/10.1038/s41598-023-41869-w

Chenna, S., Koopman, W. J. H., Prehn, J. H. M., & Connolly, N. M. C. (2022). Mechanisms and mathematical modeling of ROS production by the mitochondrial electron transport chain. *Am. J. Physiol. - Cell Physiol.*, *1*, C69–C83. https://doi.org/10.1152/ajpcell.00455.2021

Cui, H., Kong, Y., & Zhang, H. (2012). Oxidative Stress, Mitochondrial Dysfunction, and Aging. *J. Signal Transduct.*, *2012*, 646354. https://doi.org/10.1155/2012/646354

Dhingra, N., Wei, L., & Zhao, X. (2019). Replication protein A (RPA) sumoylation positively influences the DNA damage checkpoint response in yeast. *J. Biol. Chem.*, *294*(8), 2690–2699. https://doi.org/10.1074/jbc.RA118.006006

Dixon, H., & Norbury, C. J. (2002). Therapeutic exploitation of checkpoint defects in cancer cells lacking p53 function. In *Cell cycle (Georgetown, Tex.)* (Vol. 1, Issue 6). https://doi.org/10.4161/cc.1.6.257

Engeland, K. (2018). Cell cycle arrest through indirect transcriptional repression by p53: I have a DREAM. In *Cell Death and Differentiation* (Vol. 25, Issue 1). https://doi.org/10.1038/cdd.2017.172

Ferrari, M., Rawal, C. C., Lodovichi, S., Vietri, M. Y., & Pellicioli, A. (2020). Rad9/53BP1 promotes DNA repair via crossover recombination by limiting the Sgs1 and Mph1 helicases. *Nat. Commun.*, *11*(1), 3181. https://doi.org/10.1038/s41467-020-16997-w

Groth, P., Ausländer, S., Majumder, M. M., Schultz, N., Johansson, F., Petermann, E., & Helleday, T. (2010). Methylated DNA Causes a Physical Block to Replication Forks Independently of Damage Signalling, O6-Methylguanine or DNA Single-Strand Breaks and Results in DNA Damage. *J. Mol. Biol.*, *402*(1), 70–82. https://doi.org/10.1016/j.jmb.2010.07.010

Guaragnella, N., Palermo, V., Galli, A., Moro, L., Mazzoni, C., & Giannattasio, S. (2014). The expanding role of yeast in cancer research and diagnosis: Insights into the function of the oncosuppressors p53 and BRCA1/2. *FEMS Yeast Res.*, *14*(1), 2–16. https://doi.org/10.1111/1567-1364.12094

Hartwell, L. H. (2002). NOBEL LECTURE: Yeast and Cancer. *Biosci. Rep.*, *22*(3–4), 373–394. https://doi.org/10.1023/a:1020918107706

Hu, Z., Liu, Y., Zhang, C., Zhao, Y., He, W., Han, L., Yang, L., Hopkins, K. M., Yang, X., Lieberman, H. B., & Hang, H. (2008). Targeted deletion of Rad9 in mouse skin keratinocytes enhances genotoxin-induced tumor development. *Cancer Res.*, *68*(14), 5552–5561. https://doi.org/10.1158/0008-5472.CAN-07-5670

Katheeja, M. N., Das, S. P., & Laha, S. (2021). The budding yeast protein Chl1p is required for delaying progression through G1/S phase after DNA damage. *Cell Div.*, *16*(1), 4. https://doi.org/10.1186/s13008-021-00072-x

Kitanovic, A., Walther, T., Loret, M. O., Holzwarth, J., Kitanovic, I., Bonowski, F., Bui, N. V., Francois, J. M., & Wölfl, S. (2009). Metabolic response to MMS-mediated DNA damage in Saccharomyces cerevisiae is

dependent on the glucose concentration in the medium. *FEMS Yeast Res.*, *9*(4), 535–551. https://doi.org/10.1111/j.1567-1364.2009.00505.x

Kurita, H., Haruta, N., Uchihashi, Y., Seto, T., & Takashima, K. (2020). Strand breaks and chemical modification of intracellular DNA induced by cold atmospheric pressure plasma irradiation. *PLoS One*, *15*(5), e0232724. https://doi.org/10.1371/journal.pone.0232724

Loret, M. O., Pedersen, L., & François, J. (2007). Revised procedures for yeast metabolites extraction: Application to a glucose pulse to carbon-limited yeast cultures, which reveals a transient activation of the purine salvage pathway. *Yeast*, *24*(1), 47–60. https://doi.org/10.1002/yea.1435

Marei, H. E., Althani, A., Afifi, N., Hasan, A., Caceci, T., Pozzoli, G., Morrione, A., Giordano, A., & Cenciarelli, C. (2021). P53 signaling in cancer progression and therapy. In *Cancer Cell International* (Vol. 21, Issue 1). https://doi.org/10.1186/s12935-021-02396-8

Mello, S. S., Valente, L. J., Raj, N., Seoane, J. A., Flowers, B. M., McClendon, J., Bieging-Rolett, K. T., Lee, J., Ivanochko, D., Kozak, M. M., Chang, D. T., Longacre, T. A., Koong, A. C., Arrowsmith, C. H., Kim, S. K., Vogel, H., Wood, L. D., Hruban, R. H., Curtis, C., & Attardi, L. D. (2017). A p53 Super-tumor Suppressor Reveals a Tumor Suppressive p53-Ptpn14-Yap Axis in Pancreatic Cancer. *Cancer Cell*, *32*(4), 460–473. https://doi.org/10.1016/j.ccell.2017.09.007

Mihoubi, W., Sahli, E., Gargouri, A., & Amiel, C. (2017). FTIR spectroscopy of whole cells for the monitoring of yeast apoptosis mediated by p53 over-expression and its suppression by Nigella sativa extracts. *PLoS One*, *12*(7), e0180680. https://doi.org/10.1371/journal.pone.0180680N avadgi-Patil, V. M., & Burgers, P. M. (2008). Yeast DNA replication protein Dpb11 activates the Mec1/ATR checkpoint kinase. *J. Biol. Chem.*, *283*(51), 35853–35859. https://doi.org/10.1074/jbc.M807435200

Pizzul, P., Casari, E., Gnugnoli, M., Rinaldi, C., Corallo, F., & Longhese, M. P. (2022). The DNA damage checkpoint: A tale from budding yeast. *Front. Genet.*, *13*. https://doi.org/10.3389/fgene.2022.995163

Ribeiro, G. F., Côrte-Real, M., & Johansson, B. (2006). Characterization of DNA damage in yeast apoptosis induced by hydrogen peroxide, acetic acid, and hyperosmotic shock. *Mol. Biol. Cell*, *17*(10), 4584–4591. https://doi.org/10.1091/mbc.E06-05-0475

Ritter, J. B., Genzel, Y., & Reichl, U. (2006). High-performance anion-exchange chromatography using on-line electrolytic eluent generation for the determination of more than 25 intermediates from energy metabolism of mammalian cells in culture. *J. Chromatogr. B Anal. Technol. Biomed. Life Sci.*, *843*(2), 216–226. https://doi.org/10.1016/j.jchromb.2006.06.004

Salmon, T. B., Evert, B. A., Song, B., & Doetsch, P. W. (2004). Biological consequences of oxidative stress-induced DNA damage in Saccharomyces cerevisiae. *Nucleic Acids Res.*, *32*(12), 3712–3723. https://doi.org/10.1093/nar/gkh696

Schwarz, L. V., Sandri, F. K., Scariot, F., Delamare, A. P. L., Valera, M. J., Carrau, F., & Echeverrigaray, S. (2023). High nitrogen concentration causes G2/M arrest in Hanseniaspora vineae. *Yeast*, *40*(12), 640–650. https://doi.org/10.1002/yea.3911

Senoo, T., Yamanaka, M., Nakamura, A., Terashita, T., Kawano, S., & Ikeda, S. (2016). Quantitative PCR for detection of DNA damage in mitochondrial DNA of the fission yeast Schizosaccharomyces pombe. *J. Microbiol. Methods*, *127*, 77–81. https://doi.org/10.1016/j.mimet.2016.05.023

Shokolenko, I., Venediktova, N., Bochkareva, A., Wilson, G. I., & Alexeyev, M. F. (2009). Oxidative stress induces degradation of

mitochondrial DNA. *Nucleic Acids Res.*, *37*(8), 2539–2548. https://doi.org/10.1093/nar/gkp100

Siler, J., Xia, B., Wong, C., Kath, M., & Bi, X. (2017). Cell cycle-dependent positive and negative functions of Fun30 chromatin remodeler in DNA damage response. *DNA Repair (Amst).*, *50*, 61–70. https://doi.org/10.1016/j.dnarep.2016.12.009

Sjölander, J. J., & Sunnerhagen, P. (2020). The fission yeast FHIT homolog affects checkpoint control of proliferation and is regulated by mitochondrial electron transport. *Cell Biol. Int.*, *44*(2), 412–423. https://doi.org/10.1002/cbin.11241

Stenberg, S., Li, J., Gjuvsland, A. B., Persson, K., Demitz-Helin, E., Gonzalez-Pena, C., Yue, J. X., Gilchrist, C., Ärengård, T., Ghiaci, P., Larsson-Berglund, L., Zackrisson, M., Smits, S., Hallin, J., Höög, J. L., Molin, M., Liti, G., Omholt, S. W., & Warringer, J. (2022). Genetically controlled mtDNA deletions prevent ROS damage by arresting oxidative phosphorylation. *Elife*, *11*, 10.7554/elife.76095. https://doi.org/10.7554/elife.76095

Van Houten, B., Woshner, V., & Santos, J. H. (2006). Role of mitochondrial DNA in toxic responses to oxidative stress. *DNA Repair (Amst).*, *5*(2), 145–152. https://doi.org/10.1016/j.dnarep.2005.03.002

van Os, N. J. H., van Deuren, M., Weemaes, C. M. R., van Gaalen, J., Hijdra, H., Taylor, A. M. R., van de Warrenburg, B. P. C., & Willemsen, M. A. A. P. (2020). Classic ataxia-telangiectasia: The phenotype of long-term survivors. *Journal of Neurology*, *267*(3). https://doi.org/10.1007/s00415-019-09641-1

Waterman, D. P., Haber, J. E., & Smolka, M. B. (2020). Checkpoint Responses to DNA Double-Strand Breaks. *Annu. Rev. Biochem.*, *89*, 103–133. https://doi.org/10.1146/annurev-biochem-011520-104722

Whalley, N. A., Walters, S., & Hammond, K. (2018). Molecular Cell Biology. In *Mol. Med. Clin.* https://doi.org/10.18772/22008014655.9

Yao, S., Feng, Y., Zhang, Y., & Feng, J. (2021). DNA damage checkpoint and repair: From the budding yeast Saccharomyces cerevisiae to the pathogenic fungus Candida albicans. *Comput. Struct. Biotechnol. J.*, *19*, 6343–6354. https://doi.org/10.1016/j.csbj.2021.11.033